Analysis of Interchannel Crosstalk in a Dispersion-Managed Analog Transmission Link

Brian S. Marks, *Member, IEEE*, Curtis R. Menyuk, *Fellow, IEEE*, Anthony L. Campillo, *Member, IEEE*, and Frank Bucholtz, *Member, IEEE*

***Abstract*—A technique for computing the effect of cross-phase modulation (XPM) on two copropagating analog channels in an optical fiber link is presented. In this approach, the interaction between the two channels is linearized by keeping the self-phase modulation (SPM) and XPM interactions in the strong optical carrier components only at lowest order and then at the next order, deriving the effect on the modulation components of both channels when the optical carrier is strong relative to the other components of the channel. In contrast to some previously suggested approaches, it is not assumed that the pump is undistorted, and therefore, this method accurately describes distortions due to SPM, XPM, and dispersion management in both channels. This method is easily applied to systems with multiple spans employing dispersion management with loss and gain. The expressions for the received radio frequency power and crosstalk between the two channels when direct detection is used are then provided. Using this approach, new expressions for the amplitude modulation and phase modulation modes of the two channels are derived, and the way they exchange energy when SPM, XPM, and dispersion are all considered is explained. This method yields excellent agreement between theory and experimental data.**

***Index Terms*—Analog transmission, cross-phase modulation (XPM), crosstalk, intensity modulation, phase modulation (PM), self-phase modulation (SPM), wavelength-division multiplexing.**

I. Introduction

In the transmission of analog signals over optical fibers, cross-phase modulation (XPM) between channels in a wavelength-division-multiplexed (WDM) system can be highly detrimental in the presence of dispersion. The effect of XPM is to transfer the intensity modulation in one channel, which we call the "pump" channel, to phase modulation (PM) in another, which we call the "probe" channel. The fiber's group-velocity dispersion then converts this PM into intensity modulation, distorting the probe channel. The resulting transfer of intensity modulation from the pump to the probe is measured by the crosstalk, which is defined as the ratio in decibels of the received radio frequency (RF) power in the probe channel to the received RF power in the pump channel at a given modulation frequency [1]–[4]. In contrast to digital transmission systems, waveform distortion in analog systems must be kept to a minimum to maintain high fidelity. A good model must therefore accurately characterize all the important sources of distortion.

Because crosstalk in an analog link arises because of the Kerr nonlinearity, it is reasonable to mitigate it by using dispersion management, which has been used successfully in digital links to reduce the nonlinear interaction between channels. In a dispersion-managed system, a large local dispersion is used to achieve a large group-velocity difference between the channels, thereby averaging the nonlinear phase rotation in the probe over many periods of the amplitude modulation (AM) in the pump. At the receiver, the fiber dispersion is compensated so that the signal incurs little dispersive distortion.

Several investigators have considered the problem of analytically calculating crosstalk in analog fiber links limited by XPM [1], [5], [6]. In some cases, closed-form expressions for the crosstalk have been presented [1], [5]. However, previous work did not include the effect of pump channel distortion during transmission, which we have found is necessary to accurately compute the crosstalk for large modulation frequencies and for the dispersion-managed experiments we are modeling. One may compute the crosstalk for any system by resorting to computationally costly numerical integration of the nonlinear Schrödinger equation. However, in this paper, we linearize the system by assuming that the modulation depth and the ratio of the modulation frequency to the channel spacing are small, yielding a linear system of ordinary differential equations (ODEs). After solving this system of ODEs, we compute the crosstalk. This linearization quantitatively captures all of the characteristics of the XPM-induced crosstalk, even in complicated systems with dispersion management and periodic gain and loss. The equations reveal the underlying physics and are computationally nearly as rapid to evaluate as earlier closed-form expressions. We validate our results by comparison to full numerical simulations and experiments.

II. Analysis

We begin our analysis with the nonlinear Schrödinger equation with z-varying dispersion, loss, and gain, which is expressed as

$$\frac{\partial Q}{\partial z} = \frac{j}{2}\beta(z)\frac{\partial^2 Q}{\partial t^2} + j\gamma|Q|^2 Q - \frac{1}{2}\Gamma(z)Q \qquad (1)$$

Manuscript received August 18, 2005; revised February 24, 2006. This work was supported in part by the U.S. Office of Naval Research.

B. S. Marks was with the Department of Computer Science and Electrical Engineering, University of Maryland Baltimore County, Baltimore, MD 21250 USA. He is now with the Department of Psychological and Brain Sciences, Indiana University, Bloomington, IN 47405 USA (e-mail: bsmarks@indiana.edu).

C. R. Menyuk is with the Department of Computer Science and Electrical Engineering, University of Maryland Baltimore County, Baltimore, MD 21250 USA.

A. L. Campillo and F. Bucholtz are with the Naval Research Laboratory, Washington, DC 20375 USA (e-mail: alc@ccs.nrl.navy.mil; bucholtz@ccs.nrl.navy.mil).

Digital Object Identifier 10.1109/JLT.2006.874558

where Q is the electric field envelope normalized so that $|Q|^2$ has the units of power, $\beta(z)$ is the z-dependent dispersion, γ is the fiber's nonlinear coefficient, and $\Gamma(z)$ is the z-dependent loss/gain. This equation may be usefully rewritten as a nonlinear Schrödinger equation with z-varying dispersive and nonlinear coefficients by making the transformation

$$q(z,t) = Q(z,t)\exp\left[\frac{1}{2}\int_0^z \Gamma(z')dz'\right] \tag{2}$$

which yields

$$\frac{\partial q}{\partial z} = \frac{j}{2}\beta(z)\frac{\partial^2 q}{\partial t^2} + jF(z)|q|^2 q \tag{3}$$

where

$$F(z) = \gamma\exp\left[-\int_0^z \Gamma(z')dz'\right]. \tag{4}$$

Equation (3) does not include the Raman effect or polarization effects; the Raman effect has a significant effect on crosstalk below a modulation frequency of 2 GHz [1]. The goal of this paper is to describe effects that occur at larger modulation frequencies, where the Kerr effect and its interaction with dispersion dominates the crosstalk.

We will begin by focusing on the case where the signal consists of two well-separated wavelength channels. By well separated, we mean that the crosstalk from the demultiplexing filters is negligible, so that all of the observable crosstalk comes from the nonlinear interaction during the propagation. In this case, we may write $q(z,t) = u(z,t) + v(z,t)\exp(j\Delta\omega t)$, where $\Delta\omega$ is the frequency spacing of the channels. Because the u and v channels are well separated, we can separately describe the evolution of each of the wavelength channels with the coupled equations [7]

$$\frac{\partial u}{\partial z} = \frac{j}{2}\beta(z)\frac{\partial^2 u}{\partial t^2} + jF(z)\left(|u|^2 + 2|v|^2\right)u \tag{5a}$$

$$\frac{\partial v}{\partial z} = \frac{j}{2}\beta(z)\left(\frac{\partial^2 v}{\partial t^2} + 2j\Delta\omega\frac{\partial v}{\partial t} - \Delta\omega^2 v\right) + jF(z)\left(2|u|^2 + |v|^2\right)v. \tag{5b}$$

We obtain these equations by substituting the expression for $q = u + v\exp(j\Delta\omega t)$ into (3) and setting the factors multiplying $\exp(jn\Delta\omega t)$ when $n = 0$ or 1 to zero.

We are interested in the transmission of only a small number of RF tones. Therefore, a Fourier decomposition of the electric fields in these tones is natural. We make this decomposition by letting

$$u(z,t) = \sum_{k=-\infty}^{\infty}\tilde{u}_k(z)\exp(jk\Omega t) \tag{6a}$$

$$v(z,t) = \sum_{k=-\infty}^{\infty}\tilde{v}_k(z)\exp\left\{jk\Omega\left[t - \Delta\omega g(z)\right]\right\} \tag{6b}$$

where $g(z) = \int_0^z \beta(z')dz'$. The Fourier decomposition for v contains the dispersion-dependent group velocity relative to that of the u channel. The Fourier decomposition yields a set of coupled ODEs, which are expressed as

$$\frac{d\tilde{u}_k}{dz} = -\frac{j}{2}\Omega^2 k^2\beta(z)\tilde{u}_k + jF(z) \times \sum_{p=-\infty}^{\infty}\sum_{n=-\infty}^{\infty}\left\{\tilde{u}_{k-p+n}\tilde{u}_n^* + 2\tilde{v}_{k-p+n}\tilde{v}_n^* \times \exp\left[-j(k-p)\Omega\Delta\omega g(z)\right]\right\}\tilde{u}_p \tag{7a}$$

$$\frac{d\tilde{v}_k}{dz} = -\frac{j}{2}(\Omega^2 k^2 + \Delta\omega^2)\beta(z)\tilde{v}_k + jF(z) \times \sum_{p=-\infty}^{\infty}\sum_{n=-\infty}^{\infty}\left\{2\tilde{u}_{k-p+n}\tilde{u}_n^*\exp\left[j(k-p)\Omega\Delta\omega g(z)\right] + \tilde{v}_{k-p+n}\tilde{v}_n^*\right\}\tilde{v}_p. \tag{7b}$$

A. Channels' Fourier Evolution

In the transmission of either AM or PM of a single RF tone, there are three tones in the optical field in each channel that are important: a strong tone corresponding to the optical carrier and two weak sidebands corresponding to the modulation. We therefore introduce a perturbation expansion of each channel [8], which is defined as

$$\begin{Bmatrix}\tilde{u}_k\\ \tilde{v}_k\end{Bmatrix} = \begin{Bmatrix}u_{0,k}\\ v_{0,k}\end{Bmatrix} + m\begin{Bmatrix}u_{1,k}\\ v_{1,k}\end{Bmatrix} + \mathcal{O}(m^2) \tag{8}$$

where m is the modulation depth, which we assume to be small. In our theory, the modulation depth m is assumed to be small enough that the power in the optical modulation tones is small compared to the power in the optical carrier (direct current) tones. We have found in full simulations that when m is less than about 0.1–0.2, it is small enough so that the theory works well. This value is consistent with what is generally the case in regular perturbation expansions [8]. The range of values over which we have verified this limit is necessarily small because full simulations are computationally expensive. Our goal is to linearize the interaction between the two channels about the optical carriers and to derive the correction to the field due to the small modulation. Therefore, we assume that $\tilde{u}_0$ and $\tilde{v}_0$ are of order 1, $\tilde{u}_{\pm1}$ and $\tilde{v}_{\pm1}$ are of order m, and all other Fourier components of the channels are of order m^2 or higher.

To leading order, we must solve for the interaction between the optical carrier tones $(k = 0)$ of the two channels. This leading-order problem is equivalent to assuming that there is no modulation in either channel. The resulting differential equations are given as follows:

$$\frac{du_{0,0}}{dz} = jF(z)\left(|u_{0,0}|^2 + 2|v_{0,0}|^2\right)u_{0,0} \tag{9a}$$

$$\frac{dv_{0,0}}{dz} = -\frac{j}{2}\Delta\omega^2\beta(z)v_{0,0} + jF(z)\left(2|u_{0,0}|^2 + |v_{0,0}|^2\right)v_{0,0}. \tag{9b}$$

These equations yield the exact solutions

$$u_{0,0}(z) = u_{0,0}(0)\exp\left[j(P_1+2P_2)h(z)\right] \tag{10a}$$

$$v_{0,0}(z) = v_{0,0}(0)\exp\left[-\frac{j}{2}\Delta\omega^2 g(z)+j(2P_1+P_2)h(z)\right] \tag{10b}$$

where $h(z)=\int_0^z F(z')dz'$, $P_1=|u_{0,0}(0)|^2$, and $P_2=|v_{0,0}(0)|^2$. Without loss of generality, we assume that the initial values $u_{0,0}(0)$ and $v_{0,0}(0)$ are real so that they simply equal $\sqrt{P_1}$ and $\sqrt{P_2}$, respectively.

At the next order in the perturbation expansion, $\mathcal{O}(m)$, we obtain four coupled differential equations for $u_{1,\pm1}$ and $v_{1,\pm1}$. Whereas simple substitution yields unwieldy differential equations, the change of variables

$$y_1(z) = u_{1,1}(z)\exp[\,j\phi_1(z)\,] \tag{11a}$$

$$y_2(z) = u^*_{1,-1}(z)\exp[\,j\phi_2(z)\,] \tag{11b}$$

$$y_3(z) = v_{1,1}(z)\exp[\,j\phi_3(z)\,] \tag{11c}$$

$$y_4(z) = v^*_{1,-1}(z)\exp[\,j\phi_4(z)\,] \tag{11d}$$

simplifies the equations significantly when we choose

$$\phi_1(z) = -(P_1+2P_2)h(z)+\frac{\Omega\Delta\omega}{2}g(z) \tag{12a}$$

$$\phi_2(z) = (P_1+2P_2)h(z)+\frac{\Omega\Delta\omega}{2}g(z) \tag{12b}$$

$$\phi_3(z) = -(2P_1+P_2)h(z)+\frac{1}{2}(\Delta\omega^2-\Omega\Delta\omega)g(z) \tag{12c}$$

$$\phi_4(z) = (2P_1+P_2)h(z)-\frac{1}{2}(\Delta\omega^2+\Omega\Delta\omega)g(z). \tag{12d}$$

With this change of variables, we now obtain the system of differential equations

$$\frac{d\mathbf{y}}{dz} = j\left[\frac{1}{2}\beta(z)\Omega\mathsf{M}+F(z)\mathsf{N}\right]\mathbf{y}(z) \tag{13}$$

where $\mathbf{y}(z)=(y_1,y_2,y_3,y_4)^T$, and M and N are constant 4×4 matrices, which are given as

$$\mathsf{M} = \begin{pmatrix} -\Omega+\Delta\omega & 0 & 0 & 0 \\ 0 & \Omega+\Delta\omega & 0 & 0 \\ 0 & 0 & -\Omega-\Delta\omega & 0 \\ 0 & 0 & 0 & \Omega-\Delta\omega \end{pmatrix} \tag{14}$$

and

$$\mathsf{N} = \begin{pmatrix} P_1 & P_1 & 2\sqrt{P_1P_2} & 2\sqrt{P_1P_2} \\ -P_1 & -P_1 & -2\sqrt{P_1P_2} & -2\sqrt{P_1P_2} \\ 2\sqrt{P_1P_2} & 2\sqrt{P_1P_2} & P_2 & P_2 \\ -2\sqrt{P_1P_2} & -2\sqrt{P_1P_2} & -P_2 & -P_2 \end{pmatrix}. \tag{15}$$

Equation (13) is a homogeneous linear system of ODEs with variable coefficients. Obtaining a general solution explicitly can only be done for special cases, but one can numerically integrate the system for any given dispersion map and gain/loss profile. Because these equations are fourth-order ODEs, the numerical evaluation is computationally rapid—far more rapid than the evaluation of the evolution of the original partial differential (1)—and can thus be used in parametric studies of the system. Additionally, the two terms in (13) separate the effects of dispersion and power variation in the variable coefficients $\beta(z)$ and $F(z)$.

B. Computing Crosstalk—Direct Detection

Once the vector $\mathbf{y}(z)$ is obtained at some distance by integrating (13), we use it to compute the crosstalk [1]–[4]. The two channels are typically transmitted in a pump–probe arrangement so that the pump channel is modulated, whereas the probe channel is of continuous wave (CW) initially. Therefore, the crosstalk is defined as [1]

$$\text{Crosstalk}(\Omega) = 10\log_{10}\left[\frac{\text{RF power of probe channel}(\Omega)}{\text{RF power of pump channel}(\Omega)}\right]. \tag{16}$$

The RF power given by an RF spectrum analyzer is computed by the square-magnitude of the complex Fourier component of the received photocurrent. Therefore, if we use direct detection with an ideal square-law photodiode, the RF power is related to the optical field on the photodetector as

$$\text{RF power}(\Omega) = R\left|\frac{K}{T}\int_0^T |u(z,t)|^2\, e^{i\Omega t}dt\right|^2 \tag{17}$$

where R is the load resistance of the RF spectrum analyzer, K is the responsivity of the photodetector, and $T=2\pi/\Omega$ is the period of the RF oscillation. A similar expression is used for the v channel, and the crosstalk expression can then be evaluated.

We can determine the RF power of each channel by substituting (6a) and (6b) into (17). For the u channel, the RF power is expressed as

$$\begin{aligned}\text{RF power of } u(\Omega) = RK^2\big[&\left(|\tilde{u}_{-1}|^2+|\tilde{u}_1|^2\right)|\tilde{u}_0|^2 \\ &+\tilde{u}_0^2\tilde{u}_1^*\tilde{u}_{-1}^*+\tilde{u}_0^{*2}\tilde{u}_1\tilde{u}_{-1}\big]\end{aligned} \tag{18}$$

where we have neglected contributions that are $\mathcal{O}(m^3)$ and higher. A similar expression holds for the v channel. By substituting our expressions for $\tilde{u}_k$ and $\tilde{v}_k$, (10a)–(11d), into (18), we obtain the expressions

$$\text{RF power of } u(\Omega) = RK^2m^2P_1\left|y_1(z)+y_2(z)\right|^2 \tag{19a}$$

$$\text{RF power of } v(\Omega) = RK^2m^2P_2\left|y_3(z)+y_4(z)\right|^2. \tag{19b}$$

From these two expressions, one can compute the crosstalk, assuming that the u channel is the probe channel and the v channel is the pump channel, by using

$$\text{Crosstalk}(\Omega) = 10\log_{10}\left[\frac{P_1\left|y_1(z)+y_2(z)\right|^2}{P_2\left|y_3(z)+y_4(z)\right|^2}\right]. \tag{20}$$

This expression for the crosstalk is a leading-order expression, and higher order corrections in m can be derived by computing higher order corrections to the expressions for RF power.

C. AM and PM Mode Evolution

Because direct detection is only capable of measuring AM, (19a) and (19b) suggest that the modes responsible for AM in the u and v channels are the sums $y_1(z)+y_2(z)$ and $y_3(z)+y_4(z)$, respectively. Indeed, if we write $u(z,t)=A(z,t)\exp[i\Phi(z,t)]$ and $v(z,t)=B(z,t)\exp[i\Theta(z,t)]$, where $A(z,t)$, $B(z,t)$, $\Phi(z,t)$, and $\Theta(z,t)$ are real functions, we find that the perturbation expansion gives to order m

$$A(z,t)=\sqrt{P_1}\left[1+m\frac{W_1(z)}{\sqrt{P_1}}\times\cos\left(\Omega t-\frac{\Omega\Delta\omega}{2}g(z)+\psi_1(z)\right)\right] \quad (21a)$$

$$\Phi(z,t)=\phi_0(z)+m\frac{W_2(z)}{\sqrt{P_1}}\times\sin\left(\Omega t-\frac{\Omega\Delta\omega}{2}g(z)+\psi_2(z)\right) \quad (21b)$$

$$B(z,t)=\sqrt{P_2}\left[1+m\frac{W_3(z)}{\sqrt{P_2}}\times\cos\left(\Omega t+\frac{\Omega\Delta\omega}{2}g(z)+\psi_3(z)\right)\right] \quad (21c)$$

$$\Theta(z,t)=\theta_0(z)+m\frac{W_4(z)}{\sqrt{P_2}}\times\sin\left(\Omega t+\frac{\Omega\Delta\omega}{2}g(z)+\psi_4(z)\right) \quad (21d)$$

where $W_k(z)$ and $\psi_k(z)$ are defined as

$$W_1(z)\exp\left[j\psi_1(z)\right]=y_1(z)+y_2(z) \quad (22a)$$

$$W_2(z)\exp\left[j\psi_2(z)\right]=y_1(z)-y_2(z) \quad (22b)$$

$$W_3(z)\exp\left[j\psi_3(z)\right]=y_3(z)+y_4(z) \quad (22c)$$

$$W_4(z)\exp\left[j\psi_4(z)\right]=y_3(z)-y_4(z) \quad (22d)$$

$\phi_0(z)=(P_1+2P_2)h(z)$, and $\theta_0(z)=-\Delta\omega^2 g(z)/2+(2P_1+P_2)h(z)$.

Note that $W_1(z)$ and $W_3(z)$ give the magnitudes of the AM of u and v, respectively, and $W_2(z)$ and $W_4(z)$ give the magnitudes of the PM of u and v, respectively. One can also obtain the evolution of the RF-phase offsets between these AM and PM modes by comparing the phases in (21a)–(21d).

Because our interest is understanding the evolution of the AM and PM modes of the optical signal, it is useful to change variables so that

$$A_u(z)=y_1(z)+y_2(z) \quad (23a)$$

$$P_u(z)=y_1(z)-y_2(z) \quad (23b)$$

$$A_v(z)=y_3(z)+y_4(z) \quad (23c)$$

$$P_v(z)=y_3(z)-y_4(z). \quad (23d)$$

Performing this change of variables leads to the new system for $\mathbf{w}(z)=(A_u,P_u,A_v,P_v)^T$, which is defined as

$$\frac{d\mathbf{w}}{dz}=j\left[\frac{1}{2}\beta(z)\Omega\mathcal{M}+2F(z)\mathcal{N}\right]\mathbf{w}(z) \quad (24)$$

where

$$\mathcal{M}=\begin{pmatrix}\Delta\omega & -\Omega & 0 & 0\\ -\Omega & \Delta\omega & 0 & 0\\ 0 & 0 & -\Delta\omega & -\Omega\\ 0 & 0 & -\Omega & -\Delta\omega\end{pmatrix} \quad (25)$$

and

$$\mathcal{N}=\begin{pmatrix}0 & 0 & 0 & 0\\ P_1 & 0 & 2\sqrt{P_1P_2} & 0\\ 0 & 0 & 0 & 0\\ 2\sqrt{P_1P_2} & 0 & P_2 & 0\end{pmatrix}. \quad (26)$$

The preceding formulas show that the PM mode of a channel is "pumped" by the AM and PM modes of the channel itself as well as the AM mode of the other channel. The AM mode of a channel is only "pumped" by the AM and PM modes of the same channel through the fiber's dispersion. The combination of these two pumping mechanisms shows, first, the transfer of AM in one channel to PM in another, and, second, the transfer of PM in a channel to AM in the same channel via dispersion.

Finally, if direct detection is used and if we assume that the u and v channels are the probe and pump channels, respectively, the expression for crosstalk is then given as follows:

$$\text{Crosstalk}(\Omega)=10\log_{10}\left[\frac{P_1\left|A_u(z)\right|^2}{P_2\left|A_v(z)\right|^2}\right]=10\log_{10}\left[\frac{P_1W_1^2(z)}{P_2W_3^2(z)}\right]. \quad (27)$$

We note that when direct detection is used, it is possible to obtain either zero crosstalk when the AM mode of the probe channel vanishes or infinite crosstalk when the AM mode of the pump channel vanishes. This concept of "infinite crosstalk" is perhaps counterintuitive. Simply stated, it means that the pump channel modulation is entirely contained within the optical phase so that a direct detection receiver will not observe it, whereas simultaneously, the probe channel has incurred some AM due to the XPM and dispersion. The definition of crosstalk in (16) therefore yields infinite results. The pump's modulation can be entirely shifted into the optical phase via dispersion alone. Because the AM and PM modes of both channels interact as given by (24), it is important to emphasize that despite the vanishing of one of the AM modes, the modulation indeed persists as a PM mode. Thus, in using direct detection, one loses information about the RF modulation. As the RF transmission is zero in the pump channel at frequencies with infinite crosstalk, a practical system would not be designed to operate at these frequencies.

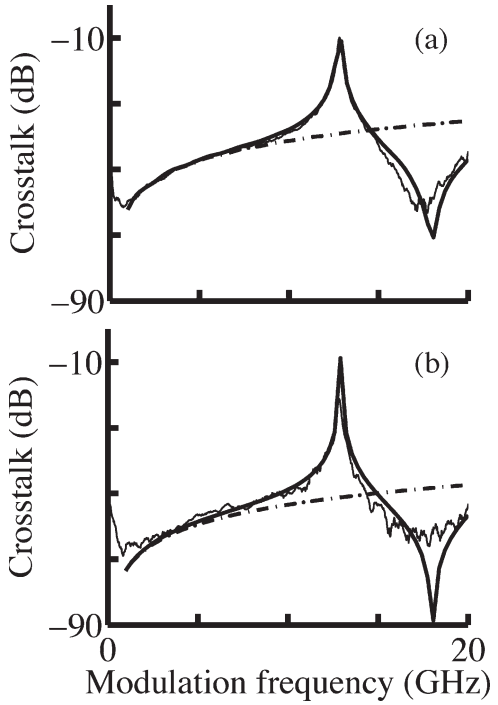

Fig. 1. Comparison between theory and experimental measurement of crosstalk for a link with constant dispersion. The pump channel wavelength was 1549.3 nm, whereas the probe channels were spaced (a) 162 GHz and (b) 995 GHz away from the pump. The thick solid curves show the results from the theory, whereas the thin solid curves show experimental data. The dot-dashed curves show the results of the theory when pump distortion is neglected.

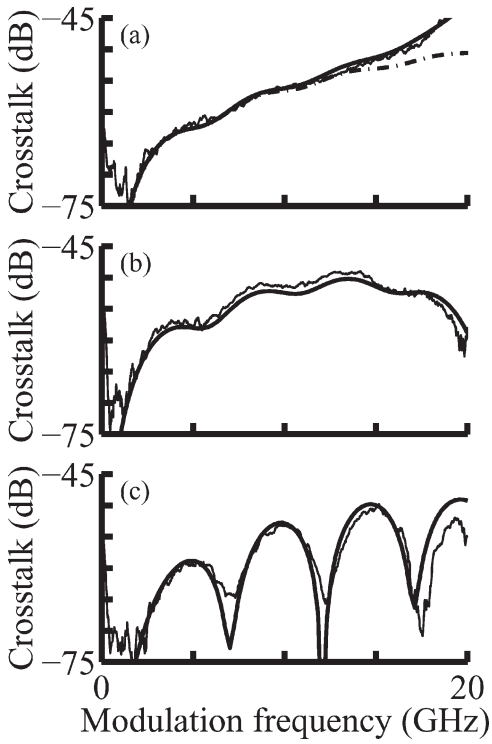

Fig. 2. Comparison between theory and experimental measurement of crosstalk for a link with dispersion-compensating fiber at the end. The dispersion-compensating fiber was cut to lengths corresponding to (a) 0%, (b) 50%, and (c) 100% of the link's accumulated dispersion. The thick solid curves show the results from the theory, whereas the thin solid curves show experimental data. The dot-dashed curve in (a) shows the result of the theory when pump distortion is neglected.

III. Results

To determine the validity of the ODE model that we use to compute the crosstalk, we have compared the results of our model with both the simulations of the full nonlinear Schrödinger equation and the experimental results. In Figs. 1 and 2, we show the results of integrating (24), first, for a system with constant dispersion and, then, for a system with dispersion-compensating fiber at the end of the transmission fiber.

Fig. 1 shows the crosstalk as a function of the modulation frequency after propagation through 25 km of Lucent AllWave fiber with $D = 17$ ps/nm-km for two different channel spacings. The fiber's nonlinear coefficient γ is specified to be 1.1 $\mathrm{W^{-1}km^{-1}}$ at 1550 nm, and the loss is 0.2 dB/km. The pump channel wavelength is 1549.3 nm, and the spacing between the pump and the probe channels was taken to be 162 GHz in Fig. 1(a) and 995 GHz in Fig. 1(b). The initial average channel power is 5 mW per channel. The thick curves indicate the results of our ODE model, whereas the thin curves show experimental data. For comparison, we also plot the simulation results when pump distortion is neglected using dot-dashed curves. The dispersion nulls shown at about 13 GHz for the pump channel and 18 GHz for the probe channel are quantitatively captured by our ODE model because both dispersive and nonlinear distortions are included in the derivation of (24) and (27). However, these nulls do not appear when the pump distortion is neglected. In addition, our ODE model does not agree with the experimental data below 2 GHz because we have neglected the Raman effect in this paper. In our model, we use a scalar nonlinear Schrödinger equation to model the propagation through the fiber. This equation implies that the pump and probe channels are in a single constant polarization state throughout propagation. If they remain copolarized, the two channels experience larger XPM than if they were cross polarized. In the experiments, the pump and probe channels were not copolarized at the input to the fiber, and, in addition, the polarization-mode dispersion in the fiber causes the two channels' polarization states to walk off relative to their respective input states. The reason for the walkoff is that the total propagation distance is equal to only a few fiber correlation lengths, and as such, there is not complete randomization of the polarization states of the two channels relative to one another. This walkoff leads to an effective reduction of the nonlinear coefficient of the fiber, which gives a single parameter for fitting our model to the experimental data. In Fig. 1, the fiber's nonlinear coefficient was reduced to 51% of its specified value of 1.1 $\mathrm{W^{-1}km^{-1}}$ in the case of the smaller channel spacing, whereas it was reduced to 77% of the specified value for the larger channel spacing.

In Fig. 2, we plot the crosstalk as a function of the modulation frequency for a dispersion-compensated system, in which we compare our ODE simulation (thick curves) and the experimental measurements of the crosstalk (thin curves) in [9]. The system used in this experiment consists of 8.1 km of Lucent UltraWave fiber followed by dispersion compensation equalling 0%, 50%, and 100% of the dispersion accumulated in the

UltraWave fiber, and the results are plotted in Fig. 2(a)–(c), respectively. The specifications of the UltraWave fiber are $D = 20$ ps/nm-km, a nonlinear coefficient γ of 0.88 $W^{-1}km^{-1}$ at 1550 nm, and a loss of $\Gamma = 0.2$ dB/km. In the simulation, we used the value $D = 15.7$ ps/nm-km for the dispersion of the 8.1-km fiber and $D = -75$ ps/nm-km for the dispersion-compensating fiber, whose length was 0 m, 850 m, and 1.7 km for the cases of 0%, 50%, and 100% dispersion compensation, respectively. We set the nonlinear coefficient γ of the dispersion-compensating fiber equal to 3.1 $W^{-1}km^{-1}$. In the experimental results of Fig. 2, care was taken to ensure that the input polarization states of the two channels were the same. In Fig. 2(a), we used 70% of the specified nonlinear coefficient of the UltraWave transmission fiber to produce the results from the simulation. In Fig. 2(b) and (c), we used exactly the specified nonlinear coefficient of the two fibers. For comparison with the result from the uncompensated link, we have plotted the XPM-induced crosstalk predicted when pump distortion is neglected (dot-dashed curve), which deviates from both the ODE simulation results and the experimental data above 13 GHz. Note that the result of (27) agrees well with both full simulations and the experimental results over the range of modulation frequency above about 2 GHz, demonstrating the importance of taking into account the pump distortion. We note that previous models of analog transmission did not take into account pump distortion and hence do not yield accurate results for the parameter regime of interest in this paper [1], [5].

IV. Conclusion

In this paper, we have derived a method for determining the XPM-induced crosstalk in an analog fiber link by solving a small system of ODEs. We have shown that a simple relationship exists between the modulation Fourier tones of the optical signal and the modes that lead to the AM and PM of the optical signal. In particular, the optical fiber converts AM to PM, and this interplay between the two can lead to nulls in the received RF power when direct detection is used. Our ODE model accurately captures these nulls in excellent agreement with the experiment. By contrast, when pump distortion is neglected as was the case in previous models, the results deviate significantly from both complete simulations and experiments, indicating that pump distortion has a significant impact on the crosstalk.

References

[1] M. R. Phillips and D. M. Ott, "Crosstalk due to optical fiber nonlinearities in WDM CATV lightwave systems," *J. Lightw. Technol.*, vol. 17, no. 10, pp. 1782–1792, Oct. 1999.

[2] F. S. Yang, M. E. Marhic, and L. G. Kazovsky, "Nonlinear crosstalk and two countermeasures in SCM-WDM communication systems," *J. Lightw. Technol.*, vol. 18, no. 4, pp. 512–520, Apr. 2000.

[3] Z. Wang, E. Bødtker, and G. Jacobsen, "Effects of cross-phase modulation in wavelength-multiplexed SCM video transmission systems," *Electron. Lett.*, vol. 31, no. 18, pp. 1591–1592, Aug. 1995.

[4] W. H. Chen and W. I. Way, "Multichannel single-sideband SCM/DWDM transmission systems," *J. Lightw. Technol.*, vol. 22, no. 7, pp. 1679–1693, Jul. 2004.

[5] R. Hui, K. R. Demarest, and C. T. Allen, "Cross-phase modulation in multispan WDM optical fiber systems," *J. Lightw. Technol.*, vol. 17, no. 6, pp. 1018–1026, Jun. 1999.

[6] A. V. T. Cartaxo, B. Wedding, and W. Idler, "Influence of fiber nonlinearity on the fiber transfer function: Theoretical and experimental analysis," *J. Lightw. Technol.*, vol. 17, no. 10, pp. 1806–1813, Oct. 1999.

[7] G. P. Agrawal, *Nonlinear Fiber Optics*, 2nd ed. New York: Academic, 1995.

[8] J. Kevorkian and J. D. Cole, *Multiple Scale and Singular Perturbation Methods*. New York: Springer-Verlag, 1996.

[9] A. L. Campillo, E. E. Funk, D. A. Tulchinsky, J. L. Dexter, and K. J. Williams, "Phase performance of an eight-channel wavelength-division-multiplexed analog-delay line," *J. Lightw. Technol.*, vol. 22, no. 2, pp. 440–447, Feb. 2004.

Brian S. Marks (M'01) was born in New Jersey in 1973. He received the B.S. degrees in mathematics and physics from North Carolina State University, Raleigh, in 1995 and the Ph.D. degree in applied mathematics from Northwestern University, Evanston, IL, in 2000.

He was a Research Associate and then a Research Assistant Professor at the University of Maryland Baltimore County, Baltimore. In 2005, he joined the Department of Psychological and Brain Sciences, Indiana University, Bloomington. His previous research interests are optimization of dispersion maps for use with dispersion-managed solitons, polarization mode dispersion, analog fiber optic communications systems, microstructure fiber modeling, and fiber amplifier modeling. His current research interests include signal and image processing in neuroimaging.

Curtis R. Menyuk (SM'88–F'98) was born on March 26, 1954. He received the B.S. and M.S. degrees from the Massachusetts Institute of Technology, Cambridge, in 1976 and the Ph.D. degree from the University of California, Los Angeles, in 1981.

He was a Research Associate at the University of Maryland, College Park, and at Science Applications International Corporation, McLean, VA. In 1986, he joined the University of Maryland Baltimore County (UMBC) as an Associate Professor in the Department of Electrical Engineering, in which he was a Founding Member. In 1993, he was promoted to Presidential Research Professor and was on partial leave from Fall 1996 to Fall 2002. From 1996 to 2001, he worked part-time for the Department of Defense (DoD), where he codirected the Optical Networking program at the DoD Laboratory for Telecommunications Sciences, Adelphi, MD, from 1999 to 2001. From 2001 to 2002, he was a Chief Scientist at PhotonEx Corporation. He has authored or coauthored more than 190 archival journal publications as well as numerous other publications and presentations and has edited three books. The equations and algorithms that he and his research group at UMBC have developed to model optical fiber systems are used extensively in the telecommunications and photonics industry. For the last 18 years, his primary research interests have been theoretical and computational studies of lasers, nonlinear optics, and fiber optic communications.

Dr. Menyuk is a member of the Society for Industrial and Applied Mathematics and the American Physical Society. He is also a Fellow of the Optical Society of America.

Anthony L. Campillo (M'03) received the B.S. and Ph.D. degrees in physics from the University of Virginia, Charlottesville, in 1996 and 2002, respectively.

He joined the Photonics Technology branch of the U.S. Naval Research Laboratory, Washington D.C., in 2001, where his research focuses on reducing nonlinear distortions in microwave photonic systems.

Dr. Campillo is a member of the Optical Society of America (OSA) and the American Physical Society (APS).

Frank Bucholtz (M'81), photograph and biography not available at the time of publication.